ChemPubSoc Europe

DOI: 10.1002/cmdc.201300355

VIP

Fluorophore-Labeled Cyclooxygenase-2 Inhibitors for the Imaging of Cyclooxygenase-2 Overexpression in Cancer: Synthesis and Biological Studies

Atul Bhardwaj,[a, b] Jatinder Kaur,[a, b] Frank Wuest,*[a] and Edward E. Knaus*[a]

A group of cyclooxygenase-2 (COX-2)-specific fluorescent cancer biomarkers were synthesized by linking the anti-inflammatory drugs ibuprofen, (*S*)-naproxen, and celecoxib to the 7-nitrobenzofurazan (NBD) fluorophore. In vitro COX-1/COX-2 inhibition studies indicated that all of these fluorescent conjugates are COX-2 inhibitors (IC_{50} range: 0.19–23.0 μM) with an appreciable COX-2 selectivity index ($SI \geq 4.3$–444). In this study the celecoxib–NBD conjugate *N*-(2-((7-nitrobenzo[*c*][1,2,5]oxadiazol-4-yl)amino)ethyl)-4-(5-(*p*-tolyl)-3-(trifluoromethyl)-1*H*-pyrazol-1-yl)benzenesulfonamide (**14**), which displayed the highest COX-2 inhibitory potency and selectivity (COX-2 $IC_{50} = 0.19$ μM; $SI = 443.6$), was identified as an impending COX-2-specific biomarker for the fluorescence imaging of cancer using a COX-2-expressing human colon cancer cell line (HCA-7).

Introduction

The high prevalence of cancer has contributed to a tremendous socioeconomic burden on healthcare systems worldwide. According to World Health Organization (WHO) statistical data in 2008, 7.6 million people died of cancer, accounting for 13% of all deaths worldwide. Recognition of the early signs (symptoms) of cancer and careful monitoring of chemotherapies can decrease cancer mortality. It is estimated that 30% of cancer deaths can be prevented. In this regard, imaging techniques have played a pivotal role in stimulating the growth and evolution of disease-specific imaging probes that can be used for selective detection of disease biomarkers. There has been a recent increase in interest in the development of molecular imaging probes that can sense the overexpression of cyclooxygenase-2 (COX-2) in cancer cells. The cyclooxygenases (COX-1 and COX-2) are key isozymes that catalyze the complex biotransformation of arachidonic acid into prostaglandins (PGs) and thromboxanes, which are ultimately responsible for many physiological and pathophysiological responses.[1,2] The COX-1 isozyme mediates homeostatic functions such as cytoprotection of the gastric mucosa, induction of labor pain, regulation of renal blood flow, and platelet aggregation. In contrast, the COX-2 isozyme is mainly responsible for the production of inflammatory PGs that induce pain, swelling, and fever.[3–5]

Traditional nonsteroidal anti-inflammatory drugs (NSAIDs) such as acetylsalicylic acid (Aspirin, **1**), (*S*)-naproxen (**2**), and ibuprofen (**3**) have broad inhibitory profiles. This nonselective inhibition that blocks the expression of both COX isozymes is responsible for their gastrointestinal (GI), ulcerogenic, hepatic, and renal toxicity.[6–10] The discovery of the inducible COX-2 isozyme in the early 1990s lent credence to the idea that selective inhibition of COX-2 would be an attractive approach for the safe treatment of inflammatory conditions. The subsequent development and US Food and Drug Administration (FDA) approval of selective COX-2 inhibitors (COXIBs, examples shown in Figure 1) provided new non-ulcerogenic drugs for the safe treatment of inflammation, arthritis, and moderate-to-severe pain.[3] Despite their initial commercial success, the selective COX-2 inhibitors rofecoxib (Vioxx) and valdecoxib (Bextra) were withdrawn from the market due to adverse cardiovascular events associated with their use.[11,12] Nitric oxide (NO)-releasing NSAIDs and selective COX-2 inhibitory prodrugs designed to circumvent adverse cardiovascular risks have now been described.[13–16]

In addition to its ability to induce peripheral inflammation, expression of the COX-2 isozyme is up-regulated in many human cancers including gastric, breast, lung, colon, esophageal, prostate, and hepatocellular carcinomas.[17–20] Many studies have shown the association between COX-2 overexpression and the development of cancer. Consequently, several COX-2 inhibitors have been investigated as anticancer agents.[21–24] It has been observed that regular intake of NSAIDs can induce apoptosis in colon carcinoma cells, retarding cancer progression.[25–27] Overall, pharmacological studies advocate that overexpression of the COX-2 isozyme in cancer cells, relative to normal neighboring tissues where COX-2 is not overexpressed, could constitute a useful noninvasive diagnostic and therapeutic strategy for the detection of cancer progression and/or treatment. These perspectives provided the impetus to investigate radioactive positron emission tomography (PET) radio-

[a] *Dr. A. Bhardwaj,[+] Dr. J. Kaur,[+] Dr. F. Wuest, Dr. E. E. Knaus*
Faculty of Pharmacy and Pharmaceutical Sciences
University of Alberta, Edmonton, Alberta, T6G 2E1 (Canada)
E-mail: wuest@ualberta.ca
eknaus@ualberta.ca

[b] *Dr. A. Bhardwaj,[+] Dr. J. Kaur[+]*
Department of Oncology, Cross Cancer Institute
University of Alberta, Edmonton, Alberta, T6G 1Z2 (Canada)

[+] *These authors contributed equally to this work.*

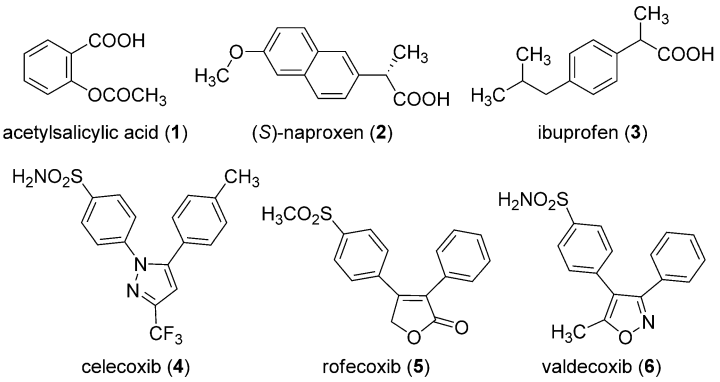

Figure 1. Representative examples of nonselective COX-1/COX-2 inhibitors **1**–**3** and selective COX-2 inhibitors **4**–**6**.

pharmaceuticals for imaging COX-2 expression; such compounds are suitable for in vivo imaging, but they require a more challenging radiosynthesis.[28,29]

Although the discovery of COX-2-specific fluorescent cancer biomarkers is still in its early stages, Marnett and colleagues recently reported that fluorescence labeling of COX-2 overexpression is a useful technique for the detection of cancer.[30] Fluorescently labeled COX-2 inhibitors are useful optical probes for targeted imaging of COX-2 in cells and small animals, as well as for clinical imaging of tissues suitable for topical or endoluminal illumination, such as the esophagus and colon. In this context, we recently reported a celecoxib–rhodamine conjugate **7**, which was investigated as a COX-2-imaging cancer biomarker.[31] Unfortunately, the weak COX-2 inhibitory potency and poor imaging results limited the use of compound **7** as a potential biomarker. As part of this ongoing program, we now describe the synthesis of a group of "fluorescent conjugates of COX inhibitors" wherein the 7-nitrobenzofurazan (NBD) fluorophore is coupled to the anti-inflammatory drugs ibuprofen, (*S*)-naproxen, and celecoxib (see structures and illustration in Figure 2) and their evaluation as in vitro COX-1 and COX-2 inhibitors, as well as their suitability as fluorescence imaging agents for the selective visualization of COX-2 activity in HCA-7 cells (COX-2-expressing human colon cancer cells).

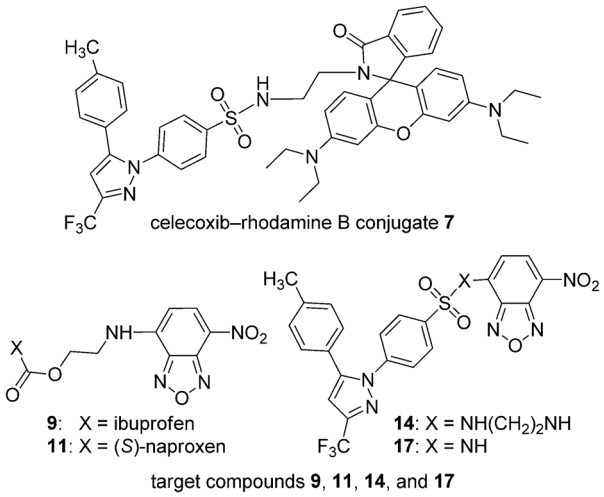

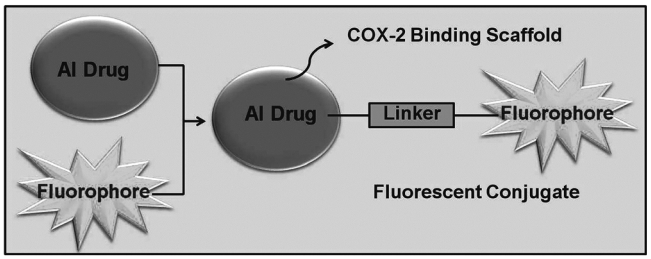

Figure 2. Structures of COX-2-inhibiting fluorescent compounds **7**, **9**, **11**, **14** and **17** (top) and a pictorial representation illustrating the design of fluorescent conjugates of COX-2 inhibitors (bottom).

Results and Discussion

Chemistry

The methods used to synthesize the target compounds **9**, **11**, **14**, and **17** are illustrated in Scheme 1. 4-Chloro-7-nitro-1,2,3-benzoxadiazole (NBD chloride, **15**) was used as a fluorophore to prepare fluorescent conjugates of the known anti-inflammatory drugs ibuprofen (compound **9**), (*S*)-naproxen (**11**), and celecoxib (**14** and **17**) through a synthetic strategy similar to that previously reported by our research group[31] (Scheme 1). Reaction of ibuprofen (**3**) or (*S*)-naproxen (**2**) with *N*-Boc-ethanolamine in the presence of *N*,*N*′-dicyclohexylcarbodiimide (DCC) and 4-dimethylaminopyridine (DMAP) in dry dichloromethane furnished the respective ester product **8** or **10**. Removal of the Boc protecting group in compounds **8** or **10** by treatment with trifluoroacetic acid (TFA) in dry dichloromethane at 25 °C afforded the respective amino product, which, without any additional purification, was allowed to react with NBD chloride in the presence of dry triethylamine (TEA) in dry THF to furnish the target ibuprofen–NBD conjugate **9** (brown solid, 64% yield, $\lambda_{em} = 548$ nm) or (*S*)-naproxen–NBD conjugate **11** (yellow solid, 62% yield, $\lambda_{em} = 555$ nm).

The 4-(5-*para*-tolyl-3-trifluoromethylpyrazol-1-yl) benzene sulfonyl chloride compound **12** was synthesized by using a previously reported synthetic methodology.[32] Condensation of this sulfonyl chloride precursor **12** with *N*-Boc-ethylenediamine in the presence of dry TEA in dry THF provided the *N*-Boc-protected celecoxib derivative **13**. The Boc protecting group was removed by treatment of **13** with TFA in dry dichloromethane to give an amino product, which, without further purification, was allowed to react with NBD chloride in the presence of dry TEA at 25 °C to furnish the celecoxib–NBD conjugate **14** ($\lambda_{em} =$ 550 nm) as a yellow solid in 69% yield.

The precursor compound 4-amino-7-nitrobenzofurazane (**16**) required for synthesis of the celecoxib–NBD conjugate **17** was prepared according to published procedures.[33,34] Reaction of NBD chloride **15** with ammonium hydroxide solution (30% in

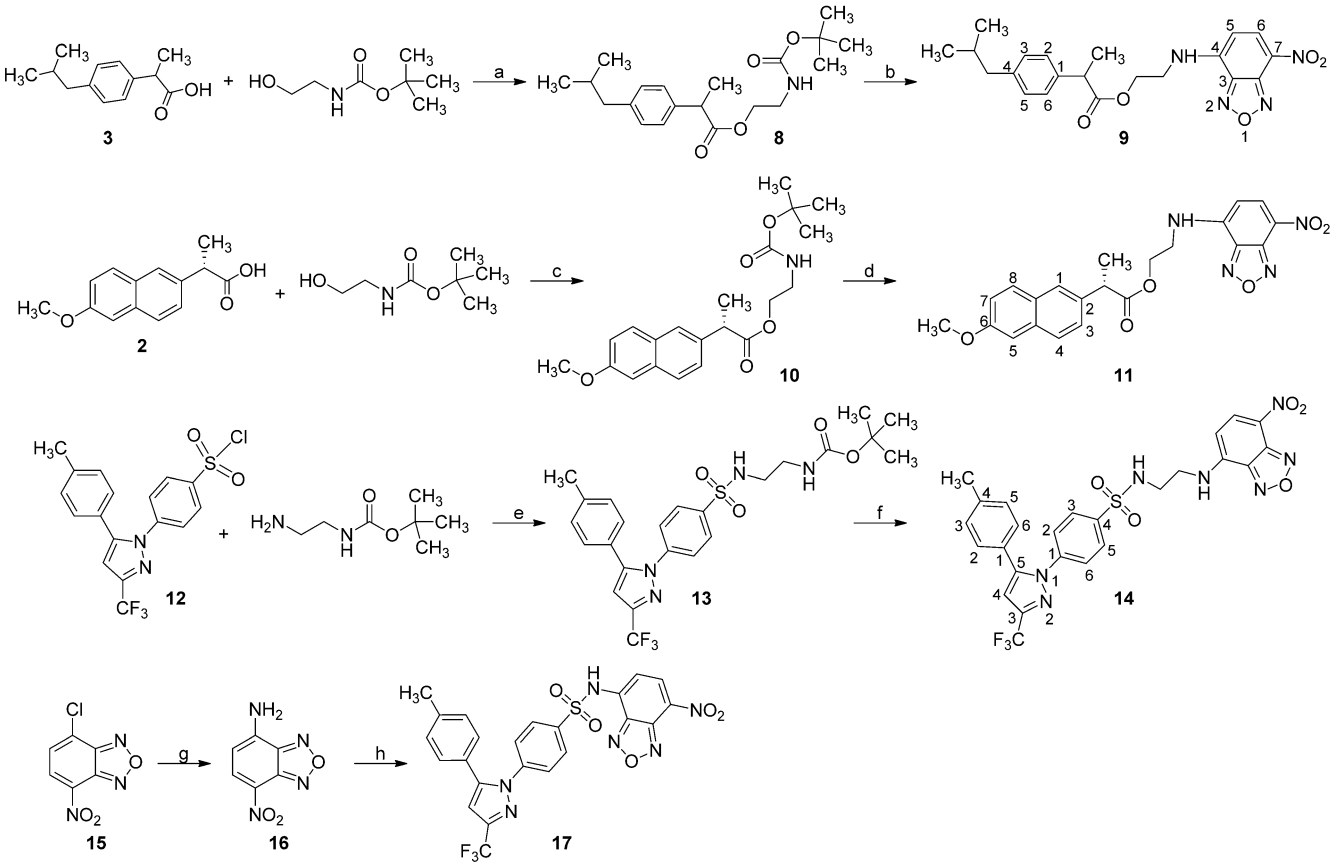

Scheme 1. *Reagents and conditions*: a), c) DCC, DMAP, dry CH_2Cl_2, 25 °C, argon atmosphere, 3 h; b), d) TFA, dry CH_2Cl_2, 25 °C, 6 h; NBD-Cl, dry TEA, dry THF, argon, 25 °C, 1 h for compound **9**, and 2 h for compound **11**; e) dry TEA, dry THF, 25 °C, 5 h; f) TFA, dry CH_2Cl_2, 25 °C, 6 h; NBD-Cl, dry TEA, dry THF, argon atmosphere, 25 °C, 30 min; g) NH_4OH solution (30% in H_2O), MeOH, 25 °C, 24 h; h) NaH, dry THF, compound **12**, 0–25 °C, 2 h.

water), with methanol as solvent, provided compound **16**. Subsequent reaction of **16** with the sulfonyl chloride analogue of celecoxib (compound **12**) in the presence of sodium hydride and dry THF afforded the target compound **17** (λ_{em} = 545 nm) as a yellow solid in 65% yield.

COX-1 and COX-2 inhibition studies

In vitro COX-1/COX-2 inhibition studies showed that compounds **9**, **11**, **14**, and **17** are more potent inhibitors of COX-2 (IC_{50} range: 0.19–23 μM) than COX-1 (IC_{50} range: 84–100 μM). Conjugates **9** and **11**, equipped with an NBD fluorophore, showed higher selectivity for COX-2 than their respective parent NSAIDs ibuprofen (**3**) or (*S*)-naproxen (**2**) (Table 1). The fluorescent ibuprofen conjugate **9** showed a higher COX-2 inhibitory activity and selectivity (COX-2 IC_{50} = 1.6 μM, SI > 62) than the (*S*)-naproxen conjugate **11** (COX-2 IC_{50} = 7.9 μM, SI = 11.7). Among the celecoxib fluorescent conjugates **14** and **17**, compound **14**, with an additional ethylamino (CH_2CH_2NH) spacer between the NBD aryl ring and the sulfonamide nitrogen, showed much higher COX-2 potency and selectivity (COX-2 IC_{50} = 0.19 μM, SI = 443.6) than compound **17**, which lacks this spacer (COX-2 IC_{50} = 23.0 μM, SI > 4.3). This ethylamino spacer is an important determinant for COX-2 inhibitory potency and selectivity (**14** > **17**). Conjugates **9** and **11**, in which the nonselective COX-1/COX-2 inhibitors ibuprofen and (*S*)-naproxen are coupled to the NBD fluorophore via an ethylamino spacer, showed greater COX-2 selectivity than the parent NSAID. This enhanced COX-2 selectivity may be attributed to the larger molecular volumes of conjugates **9** (370.1 Å^3) and **11** (353.9 Å^3) relative to the parent NSAIDs ibuprofen (211.2 Å^3) and (*S*)-naproxen (214.0 Å^3) (Table 1). Accordingly, the larger size of the ibuprofen–NBD and (*S*)-naproxen–NBD conjugates **9** and **11** may hinder their entry into the smaller COX-1 binding site (V = 316 Å^3) relative to the COX-2 binding site, which is ~25% larger (V = 394 Å^3), resulting in a higher COX-2 selectivity index.[35]

Celecoxib–NBD conjugates **14** and **17** are less potent inhibitors of COX-2 than the parent drug celecoxib (**4**, COX-2 IC_{50} = 0.07 μM). The X-ray crystal structure of celecoxib bound to the COX-2 isozyme indicates that the SO_2NH_2 COX-2 pharmacophore inserts deep into the secondary pocket of the COX-2 binding site, suggesting that this may be an important determinant of its high COX-2 inhibitory potency and selectivity.

The direct attachment of the bulky fluorescent NBD group to the sulfonamide nitrogen in conjugate **17** has a deleterious effect on COX-2 potency and selectivity (COX-2 IC_{50} = 23 μM, SI > 4.3) relative to the parent celecoxib, which has a free sulfonamide group. In comparison, conjugate **14**, with an ethylamino spacer between the sulfonamide nitrogen atom and

Table 1. In vitro COX-1 and COX-2 isozyme inhibition, molecular volume, and log *P* data.

Compd	Structure	IC_{50} [μM][a] COX-1	COX-2	SI[b]	*V* [Å^3][c]	log *P*[d]
9	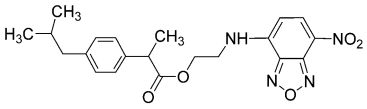	>100	1.6	>62.5	370.1	4.7
11	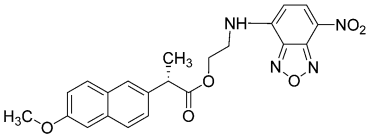	92.5	7.9	11.7	353.9	4.7
14	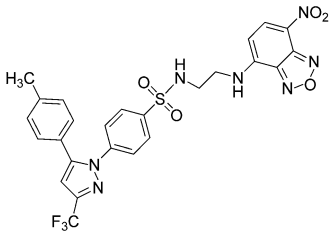	84.3	0.19	443.6	457.7	5.2
17	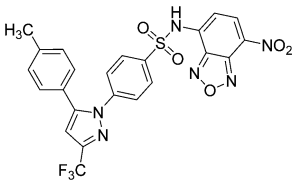	>100	23.0	>4.3	411.7	5.5
7[31]	celecoxib–rhodamine B conjugate	>100	3.9	>25.5	714.5	8.6
3	ibuprofen	2.9	1.1	2.6	211.2	3.4
2	(*S*)-naproxen	0.18	12.4	0.01	214.0	3.3
4	celecoxib	7.7	0.07	110	298.6	3.6

[a] In vitro concentration of test compound required to produce 50% inhibition of ovine COX-1 or human recombinant COX-2; results are the average of two determinations acquired using an enzyme immunoassay kit (cat. no. 560131, Cayman Chemicals Inc., Ann Arbor, MI, USA), and the deviation from the mean is <10% of the mean value. [b] In vitro COX-2 selectivity index (COX-1 IC_{50}/COX-2 IC_{50}). [c, d] Volume and log *P* of all molecules were calculated using Molinspiration Cheminformatics software (http://www.molinspiration.com).

the NBD moiety, retained high COX-2 inhibitory potency and selectivity (IC_{50} = 0.19 μM, SI = 443). These differences in COX-2 inhibitory potency and selectivity between conjugates **14** and **17** suggest that there are important differences in their binding interaction with residues in the COX-2 binding site. Log *P* molecular property calculations indicated that conjugates **9** (log *P* = 4.7), **11** (log *P* = 4.7), **14** (log *P* = 5.2), and **17** (log *P* = 5.5) are much more lipophilic than ibuprofen (log *P* = 3.4), (*S*)-naproxen (log *P* = 3.3), and celecoxib (log *P* = 3.6), as illustrated in Table 1.

Fluorescence imaging of COX-2 expression in HCA-7 colon cancer cells

Within the group of four fluorescent conjugates (**9**, **11**, **14**, and **17**), the celecoxib–NBD conjugate **14** was selected for fluorescence imaging investigations based on its appreciable in vitro COX-2 inhibitory potency. A fluorescence labeling experiment was performed with HCA-7 cells (COX-2-expressing human colon cancer cells). 4,6-Diamidino-2-phenylindole (DAPI) was used as a nucleus-specific stain. HCA-7 cells were incubated with 10 μM celecoxib–NBD conjugate **14** at 37 °C and imaged by confocal microscopy. Good cellular uptake of conjugate **14** was observed in COX-2-overexpressing HCA-7 cells (Figure 3b–d). No fluorescence was observed after incubation of HCA-7 cells with phosphate-buffered saline (PBS) control (Figure 3a) or NBD-Cl (Figure 3f) under similar experimental conditions. Pretreatment of HCA-7 cells with the potent and selective COX-2 inhibitor celecoxib (**4**) at 100 μM blocked the uptake of the celecoxib–NBD conjugate **14** by HCA-7 cells (Figure 3e), and no fluorescence labeling of the COX-2 isozyme was observed. The results of these imaging experiments indicate that HCA-7 cells, which express high levels of COX-2, exhibited strong fluorescence labeling by the celecoxib–NBD conjugate **14** at a concentration of 10 μM. This new lead compound **14** shows significant improvements in COX-2 selectivity and fluorescence imaging properties relative to conjugate **7**, previously reported.[31] A control study performed using COX-2-negative HCT-116 cells validated the hypothesis that the fluorescence imaging of COX-2 expression in HCA-7 colon cancer cells with **14** is mediated by COX-2.

Fluorescence imaging with COX-2-negative HCT-116 cells

To determine whether the fluorescence labeling of compound **14** depends on COX-2 isozyme expression, a cellular uptake experiment with HCT-116 (COX-2-negative human colon cancer) cells was performed. DAPI was used as nuclear stain. HCT-116 cells were incubated with compound **14** at either 10 or 100 μM at 37 °C prior to imaging by confocal microscopy. Importantly, no labeling was observed at either concentration of compound **14** (Figure 4b, c), and as expected, no fluorescence labeling was observed after incubation with PBS control (Figure 4a). These results indicate that the uptake of celecoxib–NBD conjugate **14** is mediated by COX-2.

Conclusions

A new group of fluorescent conjugates wherein the nonselective COX-1/COX-2 inhibitors ibuprofen and (*S*)-naproxen, or selective COX-2 inhibitor celecoxib, were coupled either directly or via an ethylamino linker group to an NBD fluorophore were

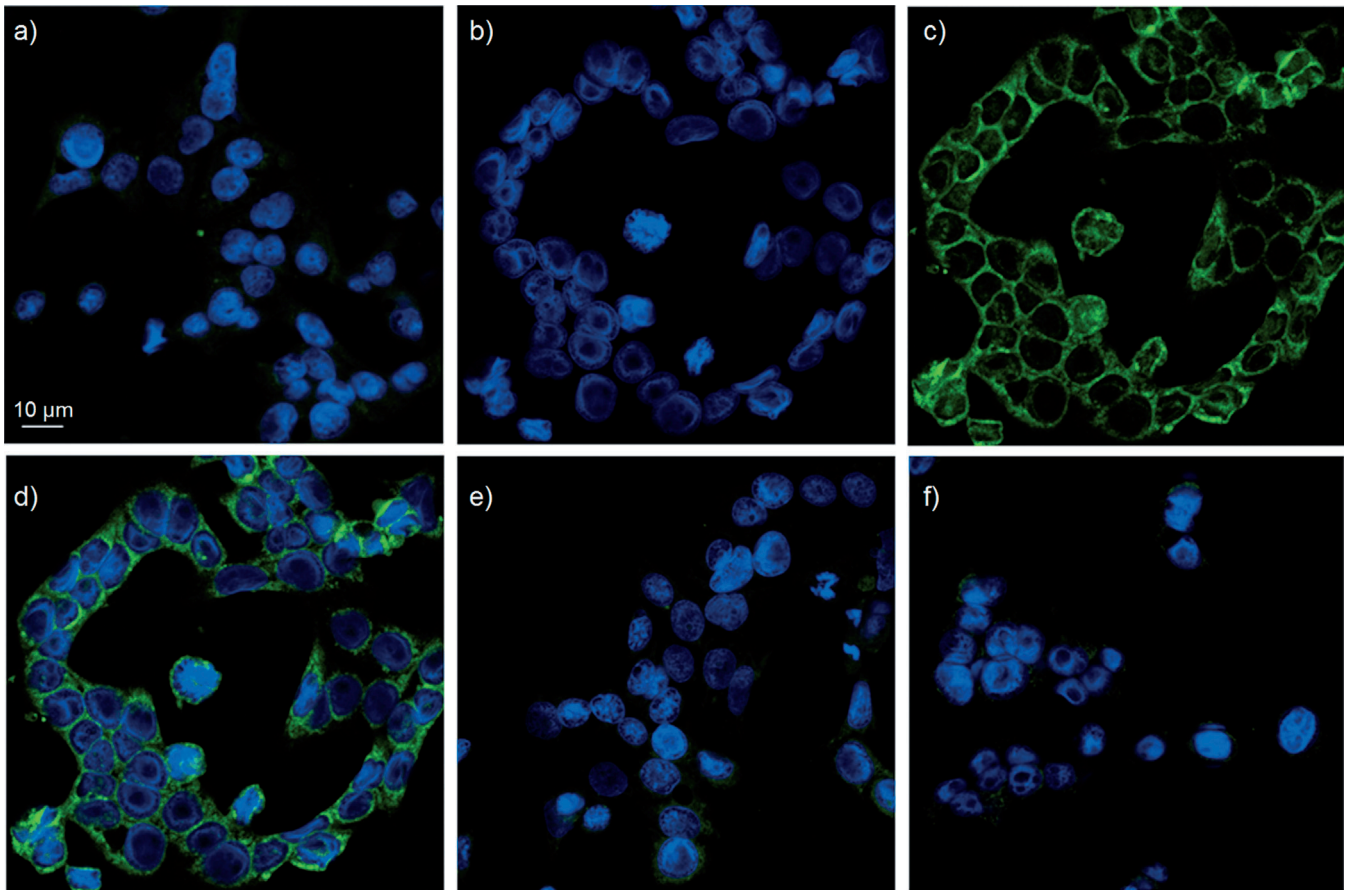

Figure 3. Fluorescence labeling of COX-2-expressing (HCA-7) cells: Cells were treated with a) PBS (control) or b)–d) 10 μM celecoxib–NBD conjugate **14**. In panel b), the stained nucleus is shown only (perinuclear staining is not shown); panel c) represents perinuclear staining due to cellular uptake of conjugate **14** (nuclear staining not shown); panel d) represents a merged image of both nuclei and perinuclear staining as a result of cellular uptake of conjugate **14**. e) Cells pre-treated with 100 μM celecoxib before treatment with conjugate **14**; f) cells treated with 10 μM NBD-Cl. Cells were imaged by confocal microscopy, and all images at the same scale as indicated in panel a).

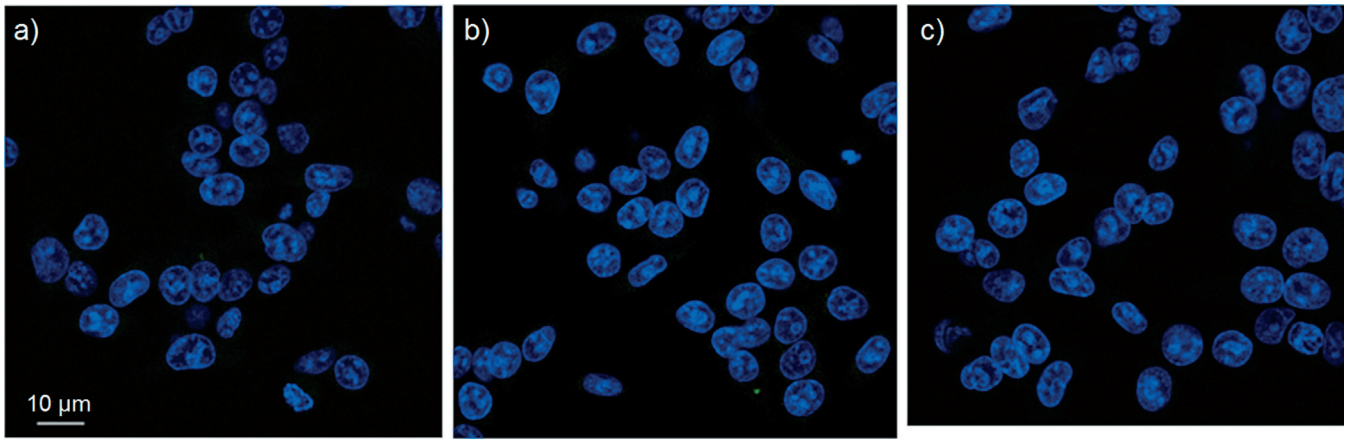

Figure 4. Uptake of compound **14** in HCT-116 cells: Cells were treated with a) PBS (control), b) 100 μM celecoxib–NBD conjugate **14**, or c) 10 μM conjugate **14**. Cells were imaged by confocal microscopy, and all images at the same scale as indicated in panel a).

synthesized for biological evaluation. In vitro COX-1/COX-2 isozyme inhibition structure–activity data showed that the ibuprofen–NBD conjugate **9** is a more selective COX-2 inhibitor than ibuprofen, the (*S*)-naproxen–NBD conjugate **11**, unlike naproxen, which is a selective COX-1 inhibitor, exhibited selective COX-2 inhibition, and the celecoxib–NBD conjugate **14** emerged as a lead compound showing the most potent COX-2 inhibitory potency and selectivity (COX-2 $IC_{50} = 0.19$ μM, SI =

443.6). Furthermore, fluorescence imaging experiments using the cancer cell lines HCA-7 (overexpressing COX-2) and HCT-116 (non-expressing COX-2) identified the celecoxib–NBD conjugate **14** as a potential fluorescence imaging agent for the labeling of overexpressed COX-2 in colon cancer cells.

Experimental Section

General

Melting points were measured with a Thomas–Hoover capillary apparatus and are uncorrected. ^{1}H and ^{13}C NMR spectra were measured on a Bruker AM 600 NMR spectrometer using $CDCl_3$ or [D_6]DMSO as solvent. Chemical shifts are given in parts per million with tetramethylsilane (TMS) as an internal reference. MS data were recorded on a Waters Micromass ZQ 4000 mass spectrometer using ESI mode. The purity of the compounds was established by elemental analyses, which were performed for C, H, and N by the Microanalytical Service Laboratory, Department of Chemistry, University of Alberta. Compounds showed a single spot on Macherey–Nagel Polygram Sil G/UV254 silica gel plates (0.2 mm) using a low, medium, and highly polar solvent system, and no residue remained after combustion, indicating a purity $>98\%$. Column chromatography was performed on a Combiflash R_f system using a gold silica column. All other reagents, purchased from the Aldrich Chemical Co. (Milwaukee, WI, USA), were used without further purification. Compounds **8**, **10**, **12**, **13**, and **16** were synthesized by using previously reported procedures.[31,32]

2-(4-Isobutylphenyl)propionic acid 2-(7-nitrobenzo-[1,2,5]oxadiazol-4-ylamino)ethyl ester (9): TFA (0.5 mL, 6.49 mmol) was added to a solution of compound **8** (500 mg, 1.43 mmol) in dry CH_2Cl_2 (10 mL), and the reaction mixture was stirred at 25 °C for 6 h. Upon completion of the reaction (TLC monitoring), excess acid and solvent was removed under vacuum, and the residue was dried in vacuo overnight. The amino product obtained, without further purification, was dissolved in dry THF (10 mL) under an argon atmosphere, and then a solution of NBD-Cl (200 mg, 1.0 mmol) in dry TEA (0.4 mL, 2.86 mmol) was added. The reaction was allowed to proceed with stirring at 25 °C for 1 h, H_2O was added, and the mixture was extracted with CH_2Cl_2 (3× 25 mL). The combined organic extracts were washed with brine prior to drying over anhydrous Na_2SO_4. Removal of the solvent in vacuo furnished a yellow liquid which was further purified by column chromatography using EtOAc/hexane (1:2, *v/v*) as eluent to give the target compound **9** in 64% yield as a brown solid; mp: 90–92 °C; ^{1}H NMR (600 MHz, $CDCl_3$): $\delta=0.77$ (d, $J=6.6$ Hz, 6H, (CH_3)$_2$CHCH$_2$), 1.41 (d, $J=7.2$ Hz, 3H, CHCH_3), 1.67–1.72 (m, 1H, (CH$_3$)$_2$C*H*CH$_2$), 2.30 (d, $J=7.2$ Hz, 2H, (CH$_3$)$_2$CHCH_2), 3.61–3.66 (m, 3H, CH$_2$CH_2NH + C*H*CH$_3$), 4.28–4.31 (m, 1H, OC*H*H′), 4.42–4.46 (m, 1H, OCH*H*′), 6.03 (d, $J=9.0$ Hz, 1H, H-5 of NBD), 6.20 (br s, 1H, N*H*), 6.93 and 7.05 (two d, $J=7.8$ Hz, 2H each, phenyl H-2, H-6 and H-3, H-5), 8.34 ppm (d, $J=9.0$ Hz, 1H, H-6 of NBD); ^{13}C NMR (150 MHz, $CDCl_3$): $\delta=18.25$ (*C*H$_3$CH), 22.30 [(*C*H$_3$)$_2$CHCH$_2$], 30.15 [*C*H(CH$_3$)$_2$], 43.02 [CH$_2$CH(CH$_3$)$_2$], 44.86 (*C*H$_2$NH), 45.03 (*C*HCH$_3$), 61.78 (OCH$_2$), 98.79 (NBD C5), 124.10 (NBD C7), 126.93 and 126.51 (phenyl *C*3, *C*5 and C2, C6), 136.10 (NBD C6), 137.02 (phenyl C1), 141.04 (phenyl C4), 143.44, 143.73 and 144.17 (NBD ArC), 174.99 ppm (CO); Fluorescence (1% DMSO in PBS): $\lambda_{em}=548$ nm; ESIMS: 411 $[M-H]^-$; Anal. calcd for $C_{21}H_{24}N_4O_5$: C 61.15, H 5.87, N 13.58, found: C 61.22, H 5.88, N 13.65.

2-(6-Methoxynaphthalen-2-yl)propionic acid 2-(7-nitrobenzo-[1,2,5]oxadiazol-4-ylamino)ethyl ester (11): TFA (0.5 mL, 6.49 mmol) was added to a solution of compound **10** (500 mg, 1.33 mmol) in dry CH_2Cl_2 (10 mL), and the reaction mixture was stirred at 25 °C for 6 h. Excess acid and solvent were removed under vacuo, and the sample was dried in vacuo overnight. The amino product obtained, without any further purification, was dissolved in dry THF (10 mL) under an argon atmosphere, and to this solution dry TEA (0.4 mL, 2.86 mmol) and NBD- Cl (220 mg, 1.1 mmol) were added. The reaction mixture was stirred at 25 °C for 1 h, H_2O was added, and the mixture was extracted with CH_2Cl_2 (3×25 mL). The combined organic extracts were washed with brine and dried over anhydrous Na_2SO_4. Removal of the solvent in vacuo furnished a yellow liquid which was further purified by column chromatography using EtOAc/hexane (1:2, *v/v*) as eluent to give the target compound **11** in 62% yield as a yellow solid; mp: 135–136 °C; ^{1}H NMR (600 MHz, $CDCl_3$): $\delta=1.48$ (d, $J=7.2$ Hz, 3H, C*H*$_3$), 3.54–3.59 (m, 2H, CH$_2$C*H*$_2$NH), 3.76–3.79 (m, 1H, C*H*CH$_3$), 3.84 (s, 3H, OC*H*$_3$), 4.21–4.25 (m, 1H, OC*H*H′), 4.54–4.58 (m, 1H, OCH*H*′), 5.77 (d, $J=9.0$ Hz, 1H, H-5 of NBD), 5.94 (br s, 1H, N*H*), 6.83 (d, $J=2.4$ Hz, 1H, naphthyl H-5), 6.97 (dd, $J=9.0$, 2.4 Hz, 1H, naphthyl H-7), 7.15 (d, $J=1.8$ Hz, 1H, naphthyl H-1), 7.36 (d, $J=8.4$ Hz, 1H, naphthyl H-4), 7.40–7.44 (m, 2H, naphthyl H-3, H-8), 8.04 ppm (d, $J=9.0$ Hz, 1H, H-6 of NBD); ^{13}C NMR (150 MHz, $CDCl_3$): $\delta=17.96$ (*C*H$_3$), 42.97 (*C*H$_2$NH), 45.36 (*C*HCH$_3$), 55.33 (OCH$_3$), 61.80 (OCH$_2$), 98.50 (NBD C5), 105.26 (naphthyl *C*5), 119.40 (naphthyl *C*7), 123.10 (NBD C7), 125.62 and 125.67 (naphthyl *C*1, *C*3), 127.16 (naphthyl *C*4), 128.52 (naphthyl Ar*C*), 128.74 (naphthyl *C*8), 133.55 and 134.78 (naphthyl Ar*C*), 135.72 (NBD C6), 143.22, 143.41 and 143.88 (NBD ArC), 157.83 (naphthyl *C*6), 174.86 ppm (CO); Fluorescence (1% DMSO in PBS): $\lambda_{em}=555$ nm; ESIMS: 437 $[M+H]^+$; Anal. calcd for $C_{22}H_{20}N_4O_6$: C 60.55, H 4.62, N 12.84, found: C 60.51, H 4.78, N 12.54; $[\alpha]^{21.0}_D=+63.54$ (0.500, $CHCl_3$).

***N*-(2-((7-Nitrobenzo[*c*][1,2,5]oxadiazol-4-yl)amino)ethyl)-4-(5-(*p*-tolyl)-3-(trifluoromethyl)-1*H*-pyrazol-1-yl)benzenesulfonamide (14)**: TFA (0.5 mL, 6.49 mmol) was added to a solution of compound **13** (500 mg, 0.95 mmol) in dry CH_2Cl_2 (10 mL), and the reaction mixture was stirred at 25 °C for 6 h. Excess TFA and solvent were removed under vacuo, and the sample was dried in vacuo overnight. The amino product obtained, without any further purification, was dissolved in dry THF (10 mL) under an argon atmosphere, and to this solution dry TEA (0.375 mL, 2.69 mmol) and NBD-Cl (200 mg, 1.0 mmol) were added. The reaction mixture was stirred at 25 °C for 30 min, H_2O was added, and the mixture was extracted with CH_2Cl_2 (3×25 mL). The combined organic extracts were washed with brine and dried over anhydrous Na_2SO_4. Removal of the solvent in vacuo furnished a yellow liquid which was further purified by column chromatography using EtOAc/hexane (1:1, *v/v*) as eluent to give the title compound **14** in 69% yield as a yellow solid; mp: 154–155 °C; ^{1}H NMR (600 MHz, [D_6]DMSO): $\delta=$ 2.29 (s, 3H, C*H*$_3$), 3.11–3.14 (m, 2H, SO$_2$NHCH_2), 3.34–3.38 (m, 2H, NHCH_2), 6.36 (d, $J=8.4$ Hz, 1H, *H*-5 of NBD), 7.19–7.21 (m, 5H, pyrazole *H*-4, 4-methylphenyl *H*-3, *H*-5, *H*-2, *H*-6), 7.55 (d, $J=8.4$ Hz, 2H, sulfonylphenyl *H*-2, *H*-6), 7.86 (d, $J=8.4$ Hz, 2H, sulfonylphenyl *H*-3, *H*-5), 8.05 (br s, 1H, N*H*), 8.53 (d, $J=8.4$ Hz, 1H, *H*-6 of NBD), 9.34 ppm (br s, 1H, N*H*); ^{13}C NMR (150 MHz, [D_6]DMSO): $\delta=20.74$ (*C*H$_3$), 40.72 (SO$_2$NHC*H*$_2$), 43.04 (*C*H$_2$NH), 99.10 (NBD C5), 106.18 (*C*H, pyrazole), 121.24 (q, $^1J_{C,F}=267$ Hz, *C*F$_3$), 121.61 (NBD C7), 125.25 (4-methylphenyl *C*1), 126.23 (sulfonylphenyl *C*2, *C*6), 127.71 (sulfonylphenyl *C*3, *C*5), 128.71 (4-methylphenyl *C*2, *C*6), 129.38 (4-methylphenyl *C*3, *C*5), 137.86 (NBD C6), 139.09 (Ar*C*), 140.14 (Ar*C*), 141.66 (Ar*C*, N-pyrazole), 142.25 (q, $^2J_{C,F}=36$ Hz, pyrazole *C*3), 144.00, 144.43 and 145.03 (NBD ArC), 145.23 ppm (pyrazole *C*5); Fluorescence (1% DMSO in PBS): $\lambda_{em}=550$ nm; ESIMS: 588 [*M*+

H]$^+$; Anal. calcd for $C_{25}H_{20}F_3N_7O_5S$: C 51.11, H 3.43, N 16.69, S 5.46, found: C 51.19, H 3.54, N 16.66, S 5.49.

***N*-(7-Nitrobenzo[*c*][1,2,5]oxadiazol-4-yl)-4-(5-(*p*-tolyl)-3-(trifluoromethyl)-1*H*-pyrazol-1-yl)benzenesulfonamide (17)**: NaH (31 mg, 1.29 mmol) was added to a solution of **16** (200 mg, 1.11 mmol) in dry THF (5 mL) at 0 °C. This solution was stirred for 15 min, compound **12** (534 mg, 1.33 mmol) in anhydrous THF (10 mL) was added dropwise, and the reaction was allowed to proceed with stirring at 25 °C for 2 h. The reaction mixture was quenched with saturated aqueous $NaHCO_3$ and extracted with EtOAc (3×25 mL). The combined organic extracts were washed with brine, dried with Na_2SO_4 and then filtered. Removal of the solvent in vacuo furnished a brown liquid which was further purified by column chromatography using EtOAc/hexane (2:1, *v*/*v*) as eluent to give the target compound **17** in 65% yield as a yellow solid; mp: 190–191 °C; ^{1}H NMR (600 MHz, [D$_6$]DMSO): δ = 2.29 (s, 3H, C*H*$_3$), 6.72 (d, *J* = 9.0 Hz, 1H, *H*-5 of NBD), 7.16–7.17 (m, 5H, pyrazole *H*-4, 4-methylphenyl *H*-3, *H*-5, *H*-2, *H*-6), 7.47 (d, *J* = 8.4 Hz, 2H, sulfonylphenyl *H*-2 and *H*-6), 7.92 (d, *J* = 8.4 Hz, 2H, sulfonylphenyl *H*-3, *H*-5), 8.35 ppm (d, *J* = 9.0 Hz, 1H, *H*-6 of NBD); ^{13}C NMR (150 MHz, [D$_6$]DMSO): δ = 21.23 (*C*H$_3$), 106.38 (NBD C5), 107.35 (*C*H, pyrazole), 121.24 (q, $^1J_{C,F}$ = 267 Hz, *C*F$_3$), 122.68 (NBD C7), 125.78 (4-methylphenyl *C*1), 126.37 (sulfonylphenyl *C*2, *C*6), 127.93 (sulfonylphenyl *C*3, *C*5), 129.18 (4-methylphenyl *C*2, *C*6), 129.85 (4-methylphenyl *C*3, *C*5), 137.18 (NBD C6), 139.50 (Ar*C*), 141.29 (Ar*C*), 142.52 (q, $^2J_{C,F}$ = 36 Hz, pyrazole *C*3), 143.81 (Ar*C*, N-pyrazole), 145.18, 145.69 and 149.38 (NBD Ar*C*), 152.34 ppm (pyrazole *C*5); Fluorescence (1% DMSO in PBS): λ_{em} = 545 nm; ESIMS: 543 [*M*−H]$^-$; Anal. calcd for $C_{23}H_{15}F_3N_6O_5S$: C 50.74, H 2.78, N 15.44, S 5.89, found: C 50.70, H 2.66, N 15.41, S 5.80.

Cyclooxygenase inhibition assays

The ability of test compounds **9**, **11**, **14**, and **17** listed in Table 1 to inhibit ovine COX-1 and human recombinant COX-2 (IC_{50} values, μM) was determined using an enzyme immunoassay (EIA) kit (cat. no. 560131, Cayman Chemical, Ann Arbor, MI, USA) according to a previously reported method.[36]

Cell culture and imaging studies

HCA-7 cells: HCA-7 colony 29 cells (Sigma–Aldrich, 02091238) were used for fluorescence imaging of COX-2 expression. The cells were cultured in T75 flasks using DMEM/F12 (1:1) medium supplemented with 10% (*v*/*v*) fetal bovine serum (FBS; Gibco, 12483), 2 mM L-glutamine (Gibco, 25030), 1% penicillin/streptomycin, and 20 mM HEPES buffer (Gibco, 15630) and were kept in a 37 °C humidified incubator with a supply of 5% CO_2 in air. After the cells were 80% confluent, they were harvested using 0.25% trypsin–EDTA (Gibco, 25200) and plated onto sterilized glass cover slips placed into a six-well cell culture plate at a density of 200000 cells per well. Cells were washed twice using PBS prior to permeabilization with 0.5% Triton X-100 in PBS (pH 7.4) for 5 min. Fixed and permeabilized cells were washed thrice with PBS before the addition of PBS as control, celecoxib–NBD conjugate **14** (10 μM), or a mixture of 100 μM celecoxib and 10 μM celecoxib–NBD conjugate to the cover slips placed in a cell culture plate, respectively. This setup was incubated at 37 °C for 30 min. Thereafter, the cells were washed with 0.1% Triton X-100 in PBS followed by three washes with PBS. All washes were for 5 min each. PBS-rinsed coverslips were then mounted onto microscopy slides using 30 μL drops of polyvinyl alcohol based mounting media supplemented with 0.1% *n*-propyl gallate as anti-fade and DAPI (50 μg mL^{-1}). The cells were imaged using corresponding lasers for visualizing DAPI (blue nuclear staining) and FITC (green emission) with a Plan-Apochromat 40X/1.3 oil DIC M27 lens on a Zeiss LSM 710 AxioObserver confocal laser scanning microscope. Imaging experiments were carried out two times using different batches of cells.

HCT-116 cells: HCT-116 cells (ATCC) were cultured at 37 °C in a humidified atmosphere of 5% CO_2 (*v*/*v*), using DMEM/F12 medium supplemented with 10% FBS (Gibco), 2 mM L-glutamine (Invitrogen), and 1% antibiotic/antimycotic (Invitrogen). Cell growth medium was changed every other day. Cells were treated with 0.25% trypsin/1 mM EDTA (Invitrogen) for ~5 min at room temperature to dissociate cells from the culture flask, and rinsed with PBS once after harvesting. Cells were resuspended in fresh growth medium and seeded into a six-well plate at 1.5×10^6 cells per well. After removing media, cells were treated with celecoxib–NBD conjugate at 100 or 10 μM using the procedure mentioned above. Imaging experiments were carried out two times using different batches of cells.

Acknowledgements

We are grateful to the Canadian Institutes of Health Research (Grant no. MOP-14712 to E.E.K.) and the Dianne and Irving Kipnes Foundation. F.W. and J.K. thank the Alberta Cancer Foundation for a postdoctoral fellowship.

Keywords: cancer · cyclooxygenases · enzymes · fluorescence · inhibitors · medicinal chemistry

[1] R. G. Kurumbail, A. M. Stevens, J. K. Gierse, J. J. McDonald, R. A. Stegeman, J. Y. Pak, D. Gildehaus, J. M. Miyashiro, T. D. Penning, K. Seibert, P. C. Isakson, W. C. Stallings, *Nature* **1996**, *384*, 644–648.
[2] L. J. Marnett, *Annu. Rev. Pharmacol. Toxicol.* **2009**, *49*, 265–290 and references therein.
[3] A. K. Chakraborti, S. K. Garg, R. Kumar, H. F. Motiwala, P. S. Jadhavar, *Curr. Med. Chem.* **2010**, *17*, 1563–1593.
[4] P. Singh, A. Mittal, *Mini-Rev. Med. Chem.* **2008**, *8*, 73–90.
[5] R. M. Langford, V. Mehta, *Biomed. Pharmacother.* **2006**, *60*, 323–328.
[6] B. Cryer, *Am. J. Gastroenterol.* **2005**, *100*, 1694–1695.
[7] M. F. Go, *Gastrointest. Endoscopy Clin. North Am.* **2006**, *16*, 83–97.
[8] M. W. James, C. J. Hawkey, *Br. J. Clin. Pharmacol.* **2003**, *56*, 146–155.
[9] G. Mounier, C. Guy, F. Berthoux, M. N. Beyens, M. Ratrema, M. Ollagnier, *Therapie* **2006**, *61*, 255–266.
[10] V. Chiroli, F. Benedini, E. Ongini, P. Del Soldato, *Eur. J. Med. Chem.* **2003**, *38*, 441–446.
[11] J.-M. Dogné, C. T. Supuran, D. Pratico, *J. Med. Chem.* **2005**, *48*, 2251–2257.
[12] T. Grosser, S. Fries, G. A. FitzGerald, *J. Clin. Invest.* **2006**, *116*, 4–15.
[13] A. Bhardwaj, S. N. Batchu, J. Kaur, Z. Huang, J. M. Seubert, E. E. Knaus, *ChemMedChem* **2012**, *7*, 1365–1368.
[14] J. Kaur, A. Bhardwaj, Z. Huang, E. E. Knaus, *ChemMedChem* **2012**, *7*, 144–150.
[15] K. Chegaev, L. Lazzarato, P. Tosco, C. Cena, E. Marini, B. Rolando, P.-A. Carrupt, R. Fruttero, A. Gasco, *J. Med. Chem.* **2007**, *50*, 1449–1457.
[16] M. N. Muscara, J. L. Wallace, *Cardiovasc. Hematol. Agents Med. Chem.* **2006**, *4*, 155–164.
[17] C. E. Eberhart, R. J. Coffey, A. Radhika, F. M. Giardiello, S. Ferrenbach, R. N. DuBois, *Gastroenterology* **1994**, *107*, 1183–1188.
[18] L. J. J. Crofford, *Rheumatology* **1997**, *49*, 15–19.
[19] A. J. Dannenberg, S. M. Lippman, J. R. Mann, K. Subbaramaiah, R. N. J. DuBois, *Clin. Oncol.* **2005**, *23*, 254–266.
[20] L. J. Marnett, R. N. DuBois, *Annu. Rev. Pharmacol. Toxicol.* **2002**, *42*, 55–80.

[21] M. Amir, H. K. Agarwal, *Pharmazie* **2005**, *60*, 563 – 570.
[22] P. Singh, A. Bhardwaj, *J. Med. Chem.* **2010**, *53*, 3707 – 3717.
[23] K. Kismet, M. T. Akay, O. Abbasoglu, E. Ercan, *Cancer Detect. Prev.* **2004**, *28*, 127 – 142.
[24] N. Pommery, T. Taverne, A. Telliez, L. Goossens, C. Charlier, J. Pommery, J. F. Goossens, R. Houssin, F. Durant, J.-P. Henichart, *J. Med. Chem.* **2004**, *47*, 6195 – 6206.
[25] T. A. Chan, *Lancet Oncol.* **2002**, *3*, 166 – 174.
[26] L. R. Howe, *Breast Cancer Res.* **2007**, *9*, 210.
[27] B. Xin, Y. Yokoyama, T. Shigeto, H. Mizunuma, *Pathol. Oncol. Res.* **2007**, *13*, 365 – 369.
[28] H. M. Schuller, G. Kabalka, G. Smith, A. Mereddy, M. Akula, M. Cekanova, *ChemMedChem* **2006**, *1*, 603 – 610.
[29] M. J. Uddin, B. C. Crews, K. Ghebreselasie, M. N. Tantawy, L. J. Marnett, *ACS Med. Chem. Lett.* **2011**, *2*, 160 – 164.
[30] M. J. Uddin, B. C. Crews, A. L. Blobaum, P. J. Kingsley, D. L. Gorden, J. O. McIntyre, L. M. Matrisian, K. Subbaramaiah, A. J. Dannenberg, D. W. Piston, L. J. Marnett, *Cancer Res.* **2010**, *70*, 3618 – 3627.
[31] A. Bhardwaj, J. Kaur, S. K. Sharma, Z. Huang, F. Wuest, E. E. Knaus, *Bioorg. Med. Chem. Lett.* **2013**, *23*, 163 – 168.
[32] G. Szabó, J. Fischer, A. Kis-Varga, K. Gyires, *J. Med. Chem.* **2008**, *51*, 142 – 147.
[33] M. Boiocchi, L. Del Boca, D. Esteban-Gomez, L. Fabbrizzi, M. Licchelli, E. Monzani, *Chem. Eur. J.* **2005**, *11*, 3097 – 3104.
[34] W. Jiang, Q. Fu, H. Fan, J. Ho, W. Wang, *Angew. Chem.* **2007**, *119*, 8597 – 8600; *Angew. Chem. Int. Ed.* **2007**, *46*, 8445 – 8448.
[35] C. Luong, A. Miller, J. Barnett, J. Chow, C. Ramesha, M. F. Browner, *Nat. Struct. Biol.* **1996**, *3*, 927 – 933.
[36] M. J. Uddin, P. N. P. Rao, R. McDonald, E. E. Knaus, *J. Med. Chem.* **2004**, *47*, 6108 – 6111.

Received: September 5, 2013
Revised: October 8, 2013
Published online on October 31, 2013